Review for CMBPol Technology Workshop, August 2008

A Review of Halfwave Plate Technology for CMB Observations circa 2008

J. E. Ruhl [1]

1. Introduction

The birefringent halfwave plate (HWP) polarization modulator, while new to the CMB field, has been used for decades at shorter wavelengths. The basic idea is simple; a polarized plane wave passing through a HWP will have its polarization orientation rotated by $\Delta\psi = 2\theta$, where θ is the angle between the incident polarization and one of the optical crystal axes. Rotating a HWP in front of a linearly polarized detector rotates the polarization sensitivity of that detector on the sky, nominally without affecting its beam pattern. This virtue, rotating polarization sensitivity without rotating a potentially asymmetric beam, is the main reason many upcoming CMB polarimeters (including ACT, Alpaca, Bicep2/Spud, Clover, EBEX, Polarbear, and Spider) will use birefringent sapphire HWP polarization modulators.

Maxipol (Johnson et al. 2007; Wu et al. 2007) is the only experiment so far to publish CMB observations using a HWP polarization modulator. With a single night of data from a balloon platform, the sensitivity was insufficient to probe B-modes, but was a good demonstration of using a HWP modulator to measure polarization on the sky.

The future use of HWPs for B-mode polarization observations will test a variety of designs and strategies for using these devices. Here we review some of the issues associated with using HWPs, and the ongoing work that will test these devices in future CMB polarization observations.

2. Major design and observing choices

There are three major design choices that each HWP implementation must make: bandwidth, operation temperature, and rotation style (continuous or stepped).

[1]Physics Department, Case Western Reserve University, Cleveland, OH 44106

The optical design of the HWP is driven by desired bandwidth. Some experiments will use separate optical paths for each observing band, with a separate HWP optimized for each. For these, the required fractional bandwidth is of order 25%. Other experiments put the HWP in an optical path that is shared by several bands; in this case, the required fractional bandwidth is much larger, of order unity. In practice, the single-band design can be simpler, using only a single-layer birefringent crystal and a single-layer anti-reflection coating. Multi-band designs require a stack of multiple birefringent plates with multilayer anti-reflection coatings. Of course all optical designs must also respect the upper limit on available diameter of materials used to construct the HWP; birefringent sapphire is available in diameters up to at least 330mm.

Most upcoming experiments are baselining cryogenic HWPs, which ensures very low thermal emission from the HWP in the observing bands and minimizes signals from reflections. However, even at 300 K the in-band emission of a single-plate sapphire HWP design is only about 2 K at 150 GHz, so ground-based experiments may be able to use ambient temperature HWPs. ACT has investigated such ambient-temperature operation (Lau 2007). The mm-wave loss in sapphire drops dramatically with temperature, so loading is unlikely to be an issue for any instrument (including CMBPol) using a cryogenic HWP.

HWPs can be used to separate beam asymmetries from polarization signals by occasional stepping of the HWP orientation or by continuously rotating it. The choice between these two strategies is intimately linked with the observing scan pattern and detector noise properties. This choice drives the mechanical design; stepper motors and conventional bearings are a good match to occasional stepping, while low heat dissipation requirements at cryogenic temperatures makes a passive magnetic bearing attractive, though perhaps not essential, for continuous rotation.

Continuous rotation comes in two flavors, which color the way one views the optical design criteria. The simplest use of a continuous rotation is to ensure the HWP modulates the polarization (at four times the HWP rotation rate f) very fast compared to rate at which the instrument's beam response is scanned across the sky. For such fast modulation, one can just lock in to the $4f$ component of the timestream and ignore other harmonics. Alternatively, one can scan across the sky fast compared to $4f$; in terms of analysis, this is much like a very rapid stepping of the waveplate.

3. Optical Designs and characterization

The coupling from a given input polarized signal to a polarized detector, as a function of photon frequency and HWP angle, can be calculated using E and H field boundary matching at each dielectric interface. An unpolarized version of this matching is worked out in matrix formulation in Hecht & Zajac (1997), while a polarized version is discussed in Savini et al. (2006). It is worth considering a few simple single-plate cases, however, to build intuition.

Case 1: When the input polarization is aligned with one of the crystal axes and the detector polarization sensitivity, the polarization is not rotated by the HWP at *any* photon frequency ν. Reflections at the various dielectric interfaces, however, will affect the transmission amplitude as a function of ν.

Case 2: Rotate the detector polarization sensitivity by 90° from Case 1. Again, the HWP does not rotate the input polarization at any ν; since the sky signal and detector sensitivity (assumed to have no crosspolar response) are crossed, there is no detector response at *any* ν. This is independent of reflections, since zero times anything is zero.

Case 3: Start with Case 1, but rotate the HWP by $\theta = 45°$. At the design frequency, the input polarization is rotated by exactly $\gamma = 2\theta = 90°$, so the detector response is zero. However, at other photon frequencies γ is not exactly 90°, so there is some detector response. This means that when the sky signal and detector sensitivity are aligned, rotating the HWP takes the band averaged signal from some large value (Case 1) to some small but non-zero value (Case 3).

Case 4: Start with Case 2, but rotate the HWP by $\theta = 45°$. At the design frequency, the input polarization is rotated by exactly $\gamma = 2\theta = 90°$, so the detector response is maximized. At nearby photon frequencies γ is not exactly 90°, so detector response is not maximized but it will still be large. This means that when the sky signal and detector sensitivity are orthogonal, rotating the HWP takes the band averaged signal from zero (Case 2) to some large value (Case 4).

Full calculations of the coupling as a function of HWP orientation angle, for normal incidence and ideal materials, generally give signals that contain a DC level, a second harmonic of the HWP rotation frequency f, and the expected signal at $4f$, the amplitudes of which are a function of photon frequency. The $2f$ signal is the result of reflections that depend on how the input signal is aligned with the crystalline axes. A figure of merit called the "polarization modulation efficiency", particularly relevant to experiments using rapidly

rotating HWPs, is unfortunately defined in different ways by different authors so we will avoid that terminology here.

The importance of various optical characteristics are driven by the desired bandwidth and the mode of operation (stepped or slow rotation vs. fast rotation). In the fast-rotation case, the $4f$ signal amplitude and phase (as a function of ν across the band) are the major parameters of interest. In the slow-rotation and stepped modes, one needs to consider the spectral response as a function of input (sky) polarization angle, for each orientation of detector sensitivity and HWP rotation angle that will be used.

3.1. Single-plate designs

A HWP constructed from a single slab of birefringent sapphire with a single-layer quarter-wave antireflection coating has a very large and uniform $4f$ signal across a 25% fractional bandwidth (top panel of Figure 1). The $2f$ signal, due to differential reflections when the input signal is aligned with the two crystal axes, is small; the DC signal is nearly the same as the $4f$ signal, indicating that the signal minima (dominated by DC + $4f$) are nearly zero. Note the absence of a $2f$ signal in the perpendicular case (Case #2 above); for the same reason, the signal minima area exactly zero, which means that the DC offset is equal to the $4f$ signal amplitude.

Several groups are building single-band, single-plate HWP systems that will be used in upcoming experiments. Our group at Case is constructing sets for Bicep2/SPUD and Spider, centered at 90, 145, 220, and 270GHz, each with about 25% fractional bandwidth. ACT, Alpaca, and Polarbear plan to use single-band, single-plate designs at 150 GHz in their first incarnations (Lau 2007; Fowler 2008; Lee 2008).

As Figure 1 illustrates, the HWP introduces features into the $4f$ amplitude bandpass of the system. These $4f$ features are independent of detector orientation relative to the sky signal, which means this can be treated just like another multiplicative effect defining the detector bandpass - there is no extra complication.

However, the $2f$ and DC features are not independent of detector orientation. For slow continuous HWP rotation, or stepped rotation, these effects must be accounted for. Figure 2 shows how this same HWP design affects sky-to-detector coupling depending on the relative angles of the sky signal, detector orientation, and HWP, for two orientations of sky signal and detector (coaligned and crossed) and four HWP orientations. The important thing to note is that in general a crossed detector pair with otherwise identical bands will have different frequency response to the same polarized sky signal. This is an extra complication that must

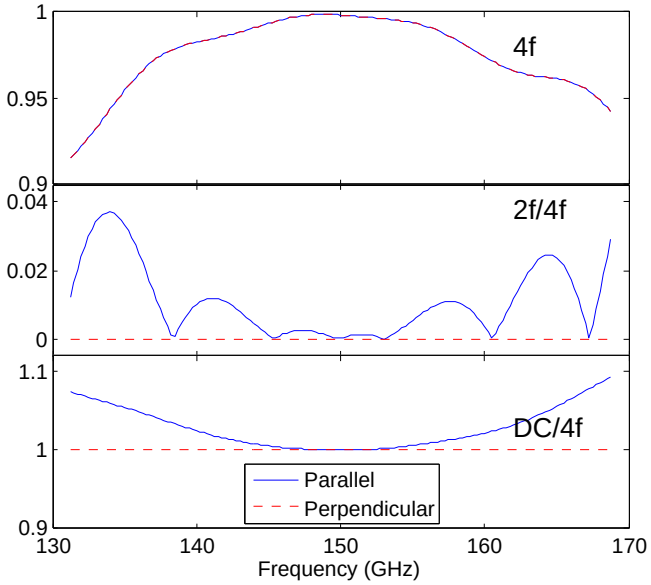

Fig. 1.— Calculated transmission signals from a completely polarized input, coupling into detectors that are sensitive to polarization parallel to (solid blue line) and perpendicular to (dashed red line) the input polarization. The top panel shows the signal that is modulated four times per HWP rotation ($4f$ component), which is the same for both plotted cases; the middle shows the ratio of the $2f$ to $4f$ (which is zero for the perpendicular case), and the bottom panel shows the ratio of the DC to $4f$, which is unity for the perpendicular case. The plotted points cover a 25% fractional bandwidth centered on 150GHz, using a single lossless sapphire waveplate ($n_s = 3.4$, $n_f = 3.07$) with an "ideal" quarter-wave AR coat that has an index $n_{AR} = \sqrt{(n_s + n_f)/2}$.

be accounted for in the data analysis.

3.2. Multi-plate designs

Multiple birefringent plates can be combined to significantly increase the useful bandwidth of the HWP (Pancharatnam 1955; Hanany et al. 2005; Pisano et al. 2006); these must be combined with wide-bandwidth anti-reflection coating to get good overall performance

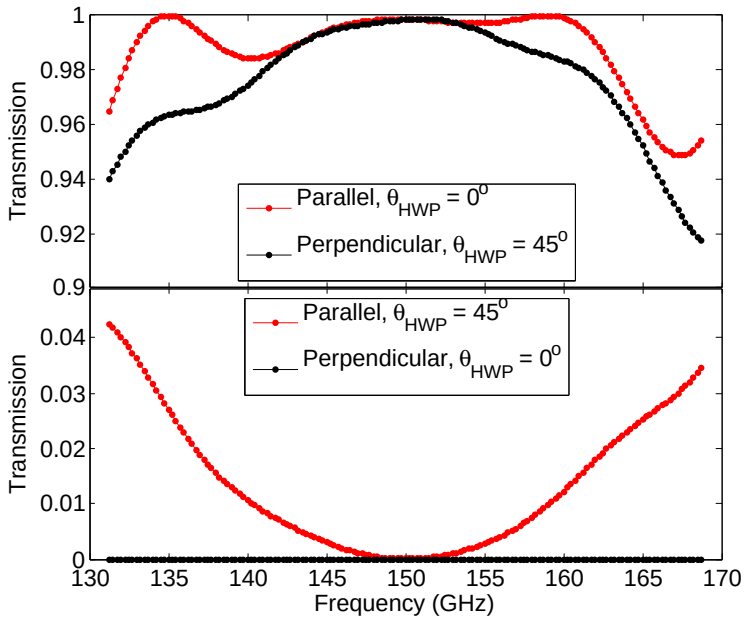

Fig. 2.— Calculated transmission as a function of photon frequency for detectors parallel (black symbols and lines) and perpendicular (red symbols and lines) to the incident polarization direction, for HWP orientations that nominally maximize (upper panel) and minimize (lower panel) those couplings. The HWP characteristics are the same as for Figure 1.

over a wide range of photon frequencies.

As an example, the calculated performance of representative a 3-plate design with a 5-layer AR coat is shown in Figure 3; with the $4f$ amplitude nearer to unity over a much larger range of photon frequencies than the single-plate design, this system enables optical designs where multiple bands share a single HWP.

Several groups are implementing multi-plate designs; Clover and EBEX are baselining them for their first observations, while other groups are considering them for use when they implement multiple bands in the future.

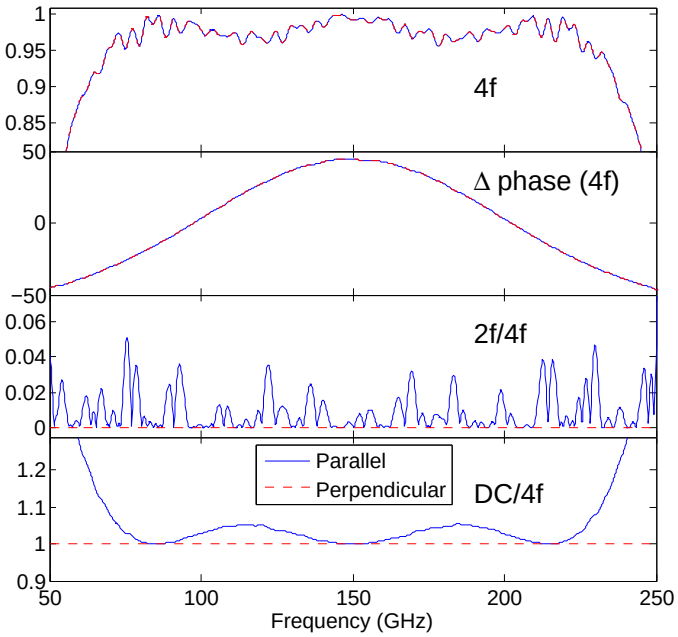

Fig. 3.— Similar to Figure 1, but for an example HWP system constructed from three birefringent sapphire plates (the middle layer is rotated by 50° with respect to the outer two laters, in this case) with a 5-layer AR coat. Here we have added another panel to the plot to show the phase difference of the $4f$ signal as a function of photon frequency, which limits the useful width of individual bands using this HWP; that is, the HWP system is still very good for multiple (narrow) bands within the frequency limits shown, but is loses efficiency for very wide bands. The reflections at the internal and external interfaces create a rich set of features in the $4f$ and $2f$ amplitudes as a function of photon frequency.

3.3. Characterization

While many experiments are planning to implement HWPs into their B-mode CMB observing instruments in the near future, there has been only a relatively small amount of detailed optical testing published so far.

The only published CMB observations with a HWP were done by Maxipol (Wu et al. 2007). That system used a single birefringent sapphire plate and single-layer AR coat, optimized for its 150 GHz observing band. Significant offsets at the HWP rotation frequency and harmonics were caused by the drive system (Johnson et al. 2003), which incorporated

a G10 shaft attached to the center of the HWP and therefore within the optical path. Despite that issue (which future implementations of HWPs for CMB observations are all avoiding), the optical performance was sufficiently good to reconstruct sky maps at the detector sensitivity limit with no obvious systematics.

The ACT team (Lau 2007) tested an ambient temperature HWP (again, single sapphire plate with a single layer AR coat) briefly installed on the CCAM instrument in Chile. Only a small amount of data was taken, but the optical performance was again promising.

Laboratory optical testing has included very narrow-band measurements using coherent sources and broadband FTS testing (Hanany et al. 2005; Pisano et al. 2006). To a large extent, this work has confirmed expectations, and has not yet raised any serious unexpected issues.

However, these tests have not yet probed all the relevant questions, such as whether spurious signals (eg from reflections) will be stable enough to avoid signal contamination, whether non-uniformities will induce systematics or degrade performance, and whether the frequency response can be characterized well enough to avoid limiting foreground subtraction. The importance of these issues is as much a function of the rest of the optical and detector system, and of the scan strategy, as they are of the HWP. We will learn an enormous amount from upcoming observations.

4. Cryogenic rotation schemes

To be useful, a HWP must be rotated (continuously or stepped) during or between observations. If the waveplate is used at 300K (as is being investigated by the ACT team), such rotation and encoding of the HWP angular position is straightforward. Rotating at cryogenic temperatures, and knowing the HWP angular position to the required level of $\approx 0.1^\circ$, is another technical challenge that must be dealt with.

4.1. Stepped rotation

Cryogenic stepped rotation is conceptually straightforward, with the caveat that linear thermal contractions must be handled. Several groups have used stepper motors at 4K to drive such motion; options range from commercially available cryo-vacuum stepper motors to simple modifications of motors built for room temperature operation. Incremental cryogenic encoders with the required precision have been constructed using cryogenic lasers, LED's, and photodiodes, and tested in the lab.

The large optical throughput of CMB polarimeters is driving a desire for larger diameter HWP's than have been used before - as large as $\sim$ 30cm clear diameter. These large diameters increase the likelihood of failure of the large diameter ball bearing assemblies (with I.D. equal to or greater than the clear aperture) used by previous designs (Rennick et al. 2002) as they thermally contract. We have built a design that avoids this problem by using three small rollers rather than one large bearing, which minimizes the likelihood of binding due to thermal contraction mismatches.

4.2. Continuous rotation

Cryogenic continuous rotation raises the issues of microphonic noise and the generation of excessive heat at those temperatures. Passive superconducting magnetic bearings (SMBs) (Hanany et al. 2003) have very low friction, and therefore minimize both microphonics and heating. Polarbear, however, will be using a standard ball-bearing at 50K, where the heat loading is less of an issue (Lee 2008).

Several drives have been developed for cryogenic, continuously rotating HWPs; EBEX will be using a magnetically levitated HWP, driven by a brushless DC motor outside the cryostat, coupled to the HWP by a shaft and a belt (Oxley et al. 2004; Hanany 2008). Polarbear is baselining a similar drive, but using standard ball bearings at the 50K HWP (Lee 2008). Here at Case, we have also prototyped and tested an integrated synchronous AC motor built into the rotor, riding on a SMB.

Knowledge of the rotation angle is of course key; as with stepped systems, encoders based on cryogenic lasers, LED's and photodiodes should provide the required precision.

5. Future Development Work

A large number of of upcoming CMB polarization experiments (eg ABS, ACT, Bicep2/SPUD, Clover, EBEX, Polarbear, and Spider) are planning to use birefringent crystal HWPs. Calculations and preliminary testing indicate that HWPs should work well for these observations. These experiments will test a wide variety of optical designs and rotation schemes, exactly as is needed to explore the usefulness of HWP polarization modulators for CMBpol.

After these upcoming experiments are done, the various HWP implementations used would be at TRL 7, defined as "System prototyping demonstration in an operational environment (ground or space)." Right now they are around TRL 4, "Component/subsystem

validation in laboratory environment". The real question for CMBPol is whether it will be using a HWP very similar to those implemented in the upcoming generation of experiments, or will require modifications; given the newness of HWPs in CMB instruments and the differences between the suborbital and orbital environments, the need for some evolution is quite likely. For this reason, it would be good to support efforts to further develop HWP concepts that specifically target issues important for their actual use in CMBPol, above and beyond the existing suborbital experiments.

REFERENCES

Fowler, J. 2008, personal communication

Hanany, S. 2008, personal communication

Hanany, S., Hubmayr, J., Johnson, B. R., Matsumura, T., Oxley, P., & Thibodeau, M. 2005, Applied Optics, 44, 4666

Hanany, S., Matsumura, T., Johnson, B., Jones, T., Hull, R., & Ma, K. B. 2003, IEEE Trans. Appl. Supercond., 13, 2128

Hecht, E. & Zajac, A. 1997, Optics (Addison Wesley)

Johnson, B. R., Abroe, M. E., Ade, P., Bock, J., Borrill, J., Collins, J. S., Ferreira, P., Hanany, S., Jaffe, A. H., Jones, T., Lee, A. T., Levinson, L., Matsumura, T., Rabii, B., Renbarger, T., Richards, P. L., Smoot, G. F., Stompor, R., Tran, H. T., & Winant, C. D. 2003, New Astronomy Review, 47, 1067, astro-ph/0308259

Johnson, B. R., Collins, J., Abroe, M. E., Ade, P. A. R., Bock, J., Borrill, J., Boscaleri, A., de Bernardis, P., Hanany, S., Jaffe, A. H., Jones, T., Lee, A. T., Levinson, L., Matsumura, T., Rabii, B., Renbarger, T., Richards, P. L., Smoot, G. F., Stompor, R., Tran, H. T., Winant, C. D., Wu, J. H. P., & Zuntz, J. 2007, ApJ, 665, 42

Lau, J. M. 2007, PhD thesis, Princeton University

Lee, A. 2008, personal communication

Oxley, P., Ade, P. A., Baccigalupi, C., deBernardis, P., Cho, H.-M., Devlin, M. J., Hanany, S., Johnson, B. R., Jones, T., Lee, A. T., Matsumura, T., Miller, A. D., Milligan, M., Renbarger, T., Spieler, H. G., Stompor, R., Tucker, G. S., & Zaldarriaga, M. 2004, in Presented at the Society of Photo-Optical Instrumentation Engineers (SPIE) Conference, Vol. 5543, Infrared Spaceborne Remote Sensing XII. Edited by Strojnik,

Marija. Proceedings of the SPIE, Volume 5543, pp. 320-331 (2004)., ed. M. Strojnik, 320–331

Pancharatnam, S. 1955, Achromatic combinations of birefringent plates, Tech. Rep. 71, Raman Research Institute, Bangalore, 137-144

Pisano, G., Savini, G., Ade, P. A. R., Haynes, V., & Gear, W. K. 2006, Applied Optics, 45, 6982

Rennick, T. S., Vaillancourt, J. E., Hildebrand, R. H., & Heimsath, S. J. 2002, in Proceedings of the 36th Aerospace Mechanisms Symposium

Savini, G., Pisano, G., & Ade, P. A. R. 2006, Applied Optics, 45(35), 8907

Wu, J. H. P., Zuntz, J., Abroe, M. E., Ade, P. A. R., Bock, J., Borrill, J., Collins, J., Hanany, S., Jaffe, A. H., Johnson, B. R., Jones, T., Lee, A. T., Matsumura, T., Rabii, B., Renbarger, T., Richards, P. L., Smoot, G. F., Stompor, R., Tran, H. T., & Winant, C. D. 2007, ApJ, 665, 55